Indian J. Phys. **72A** (4), 307–312 (1998)

IJP A
— an international journal

Defect characterization of Sr^{2+} doped calcium tartrate tetrahydrate crystals

K Suryanarayana and S M Dharmaprakash
Department of Physics, Mangalore University, Mangalagangotri-574 199, Karnataka, India

Received 12 February 1998, accepted 2 April 1998

Abstract : The defect content of gel grown Sr^{2+} doped calcium tartrate tetrahydrate single crystals (CST) with molecular formula $Ca_{0.88}Sr_{0.12}C_4H_4O_6.4H_2O$, was estimated by dislocation etching. The study revealed the existance of dislocation network in the body of the crystal. CST crystal has only one easy cleavage plane (110). The kinetics of etching is studied. From Arrhenius plots, the activation energy of etching and the pre-exponential factors are computed. An empirical relation governing the kinetics has been suggested.

Keywords : Defect characterization, etching, calcium tartrate tetrahydrate crystal

PACS Nos. : 61.72.Ff, 81.65.Cf

1. Introduction

An etching technique, in association with optical microscopy, can be used alternatively to X-ray methods for the detection as well as quantitative and qualitative analysis of defects in crystalline solids [1–5]. The segregation of foreign solute particles during crystal growth leads to the introduction of defects into the crystal [6,7]. In order to study the effect of doping of Sr^{2+} on defect characteristics and to compare the dislocations in pure and doped crystals, CST single crystals were grown in gels [8]. The characterization of CST single crystals by selective etching and a study of the kinetics of etching are reported here for the first time.

2. Experimental

CST single crystals, to be employed for etching studies, were carefully picked up from the silica gel to avoid any damage during mechanical handling. The crystal morphology was generally a rhombic octahedron (Figure 1), elongated in the *c* direction and made up of

principal faces (110), (010), (011) and their symmetry equivalants. The crystals were cleaved by light pressing with a blade parallel to (110) plane which proved to be the only possible cleavage. A number of analaR grade chemical reagents were examined for possible use as dislocation etchants. HCl and HNO_3 were found suitable etchants for CST crystals.

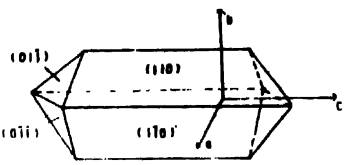

Figure 1. Morphology of Sr^{2+} doped calcium tartrate tetrahydrate single crystal.

Etch pit size was determined by taking an average of measurements on a number of etch pits at a constant magnification using a filar micrometer eye piece fitted to the optical microscope (Leitz-Wetzlar 307-002). In order to ascertain the scope of the etchants used here in delineating the linear defects existing in the body of the crystal, microscopic examinations were made of the etched mirrer cleavages and the successively etched faces. In order to test whether the etch pits are produced at the emergent sites of dislocations, successive etching was tried with each of the etchants. The etch pattern obtained on the complementary faces of CST crystal showed one to one correspondance of the etch pits on the two match halves. This indicates that the pits observed are formed at the sites of linear defects, terminal ends of which lie on both of the match surfaces. The successive etching resulted in pit widening and deepening for all etchants, thus establishing the reliability of etchants. Crystals were etched at different temperatures between room temperature and 50°C. Etch rates for different composition of the etchants was calculated from a number of measurements of the pit size.

3. Results and discussion

Figures 2 and 3 depict typical etch patterns produced on the habit faces of CST single crystals by HCl and HNO_3 respectively after etching for 10 secs. It can be seen from these figures that the etch pit morphology is independent of the nature of etchant used. Some shallow pits on the etched planes have been observed. Micropits are also found, which indicate the general dissolution of the surface, because point defects are too sensitive to etching. Such shallow and micropits formed during etching need not necessarily be related to the sites of dislocation intersection with the surface. Point defect clusters, impurity inclusions, surface damage, foreign particles on the surface and other often nontraceable factors may also lead to the formation of pits on the habit faces. Some of the etch pits on the surface are not of the same size and depth. The time lag in the formation of pits is responsible for the non-uniform size of etch pits. When the etchant attacks the dislocation sites, the pits thus formed will follow the dislocation lines into the body of the crystal. If the dislocation lines are perpendicular to the face, symmetric pits will be produced [9]. On the other hand, for inclined dislocation lines, asymmetric pits will result. When a series

Plate I

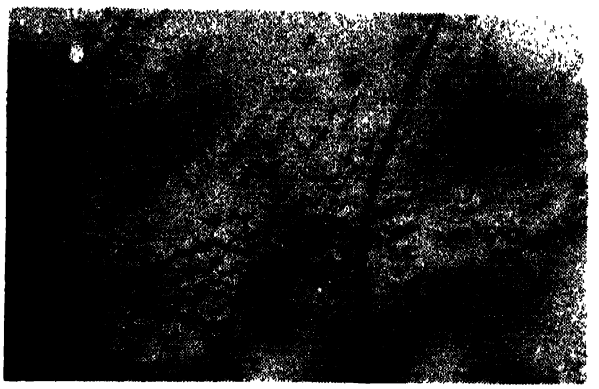

Figure 2. Etch pattern produced by HNO_3 (10 sec)

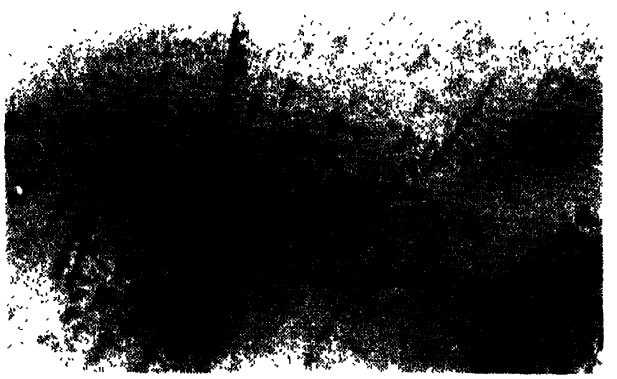

Figure 3. Etch pattern produced by HCl (10 sec)

of dislocations lying in the same slip plane meet a barrier such as a grain boundary, the dislocation pile-up takes place. The row of etch pits shown in the Figure 3 represents such an example of pile-up. The morphology and orientation of etch patterns are identical and mutually inverse. So the etch pattern symmetry on all faces is 1 m [4,10]. This accounts for the centro symmetric characteristics of CST crystal.

From the distribution of etch pits on the etched surfaces, it is observed that the dislocation density in CST single crystal is greater than the dislocation density in calcium tartrate tetrahydrate single crystals. The values of the estimated dislocation densities are of the order of 9×10^2 cm^{-2} in CST whereas in calcium tartrate tetrahydrate crystals, they are 6×10^2 cm^{-2}. The etching experiments revealed that around some foreign particles incorporated during growth of the crystals, are associated a large number of dislocations. The presence of such foreign particles may be the chief source of dislocation centres in doped crystals.

The successive etching experiments reveal that the depth and lateral size of pits increase with etching time. For quantitative analysis, the pit widths were measured at different intervals of time. The growth of pits was linearly related with time, revealing greater etch rate with greater etch concentration, suggesting the consistancy of the rate of etching.

It was observed that the concentration and temperature of the etchant have considerable influence on the etch rates. Tuck [11] suggested that the factors controlling the etching rate can be conveniently divided into two main groups : (a) those for which the rate limiting process is some aspect of chemical reaction and (b) those for which diffusion of atoms to or from the surface controls the rate. Whether the etching process is chemically controlled, can be ascertained reliably by determining etch rates as a function of temperature.

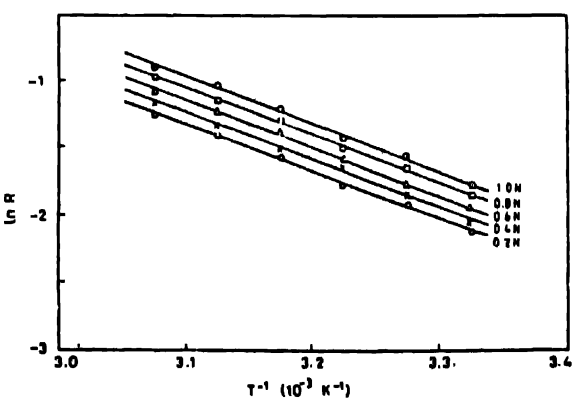

Figure 4. Plot of ln*R* against temperature for HCl.

As a rule, the dissolution process controlled by reaction rate requires an activation energy in the range 1 to 3 eV [11], while the activation energy of dissolution is limited by

diffusion change in the interval of 0.1–0.5 eV [12]. Figures 4 and 5 show Arrehenius plots of etch rates at different temperatures in the interval of 30 to 50°C for different concentrations of the etchants used. From these plots, values of activation energy and pre-exponential factors were determined and are presented in Table 1. Interestingly the values

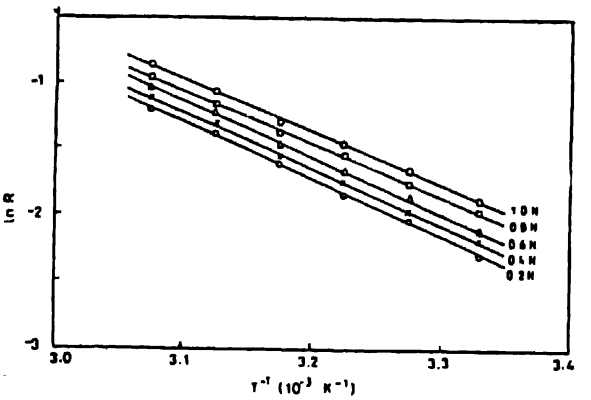

Figure 5. Plot of ln$R$ against temperature for HNO_3.

of activation energy are independent of acid concentration and lie within the limits of the reactions in which the diffusion process is predominant.

Table 1. Activation energy E (eV) and pre-exponential factors A calculated from Arrehnius plots.

Dislocation etchants	Etchant concentration	Activation energy (eV)	Arrehnius pre-exponential factor
HCl	0.2 N	0.291	8.65×10^3
	0.4 N	0.289	10.30×10^3
	0.6 N	0.296	11.38×10^3
	0.8 N	0.293	12.33×10^3
	1.0 N	0.288	12.97×10^3
HNO_3	0.2 N	0.369	12.56×10^4
	0.4 N	0.366	13.59×10^4
	0.6 N	0.362	14.16×10^4
	0.8 N	0.365	15.78×10^4
	1.0 N	0.360	16.79×10^4

The acid etchants HCl and NHO_3 react with CST, yielding tartaric acid and calcium strontium nitrate/chloride. Here, both the reaction products are water soluble. This reaction is of special interest because the exact reversal of this reaction was employed for the crystal growth of CST described elsewhere. Hence the etching process is reaction-rate controlled. No change in morphology and orientation of the pits is observed due to change

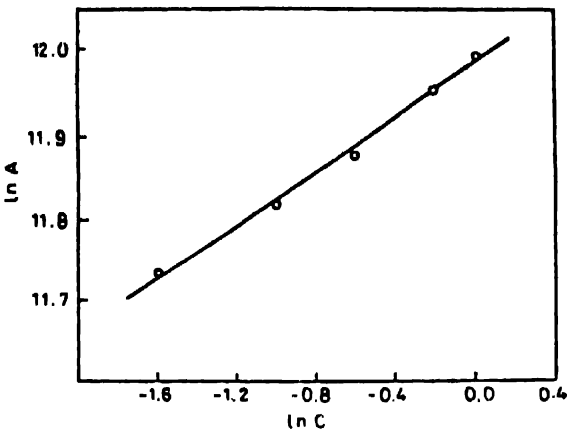

Figure 6. Plot of ln*A* against ln*C* for HNO_3.

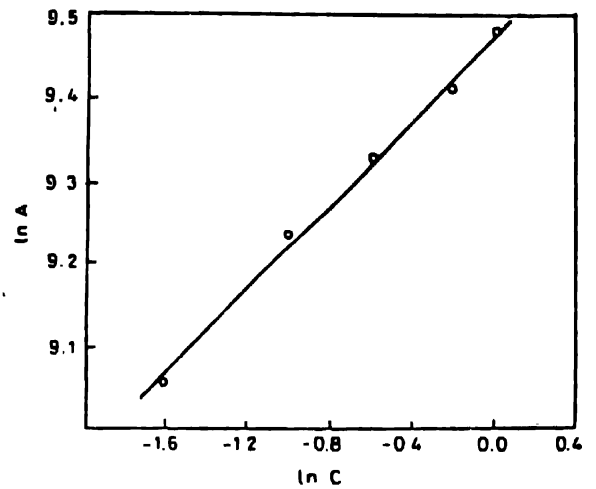

Figure 7. Plot of ln*A* against ln*C* for HCl.

in temperature. Figures 6 and 7 is the graph of ln*A* against ln*C*, from which *A* can be expressed by the empirical relations :

$$A = 12.3 \times 10^4 C^{0.16}$$

and $$A = 8.6 \times 10^3 C^{0.16}$$

for HNO_3 and HCl respectively. This enables us to represent the dissolution of CST crystals by writing the Arrhenius equation in the form

$$R = 12.3 \times 10^4 C^{0.16} \exp(-E/kT) \qquad \text{for } HNO_3$$

$$R = 8.6 \times 10^3 C^{0.16} \exp(-E/kT) \qquad \text{for HCl}$$

where *C* is the etch concentration.

4. Conclusions

CST crystal has only one easy cleavage plane (110). The etch pattern obtained on the complementary faces of CST crystal showed one to one correspondence of the etch pits on the two match halves. The successive etching resulted in pit widening and deepening, thus establishing the reliability of HCl and HNO_3 as suitable etchants for CST. The morphology and orientation of etch patterns on opposite surfaces of CST are identical and mutually inverse thus establishing the point group of CST as nonpolar 222. No change in morphology and orientation of the etch pits is observed due to change in temperature. The mechanism of etching of CST in etchants HCl and HNO_3 is reaction-rate controlled.

References

[1] J J Gilman and W G Johnston *J. Appl. Phys.* **27** 1018 (1956)

[2] V Venkataramanan, G Dhanaraj, V K Wadhawan, J N Sherwood and H L Bhat *J. Crystal Growth* **154** 92 (1995)

[3] F J Rethinam, D Arivuoli, S Ramasamy and P Ramasamy *Mater. Res. Bull.* **29** 309 (1994)

[4] N Nakatani *Japanese J. Appl. Phys.* **L1961** 30 (1991)

[5] I Owczarek and K Sangwal *J. Mater. Sci. Lett.* **9** 440 (1990)

[6] V B Paritskii, S V Lubenets and V I Startsev *Sov. Phys. Solid State* **8** 976 (1966)

[7] J J Gilman, W G Johnston and G W Sears *J. Appl. Phys.* **29** 747 (1958)

[8] K Suryanarayana and S M Dharmaprakash *Cryst. Res. & Tech.* **31** K16 (1996)

[9] A R Patel *Physica* **27** 1097 (1961)

[10] *International Table for X-ray Crystallography* eds. N F M Henry and K Lousdale (Birmingham The Kynoch Press) **Vol 1** Chap 3 (1969)

[11] B Tuck *J. Mater. Sci.* **10** 321 (1975)

[12] K Sangwal and S K Arora *J. Mater. Sci.* **13** 1977 (1978)

[13] *Kratkaya Khimicheskaya Entsiklopediya Soviet Entsiklopediya (Moscow)* V 5 (1967)